proceedings

MDPI

Proceedings

Quark Number Susceptibilities and Equation of State in QCD at Finite μ_B †

Saumen Datta *, Rajiv V. Gavai and Sourendu Gupta

Department of Theoretical Physics, Tata Institute of Fundamental Research, Homi Bhabha Road, Mumbai 400005, India; gavai@theory.tifr.res.in (R.V.G.); sgupta@theory.tifr.res.in (S.G.)

* Correspondence: saumen@theory.tifr.res.in; Tel.: +91-22-22782206

† Presented at the 7th International Conference on New Frontiers in Physics (ICNFP 2018), Crete, Greece, 4–12 July 2018.

Published: 3 June 2019

check for updates

Abstract: One of the main goals of the cold baryonic matter (CBM) experiment at FAIR is to explore the phases of strongly interacting matter at finite temperature and baryon chemical potential μ_B. The equation of state of quantum chromodynamics (QCD) at $\mu_B > 0$ is an essential input for the CBM experiment, as well as for the beam energy scan in the Relativistic Heavy Ion Collider(RHIC) experiment. Unfortunately, it is highly nontrivial to calculate the equation of state directly from QCD: numerical Monte Carlo studies on lattice are not useful at finite μ_B. Using the method of Taylor expansion in chemical potential, we estimate the equation of state, namely the baryon number density and its contribution to the pressure, for two-flavor QCD at moderate μ_B. We also study the quark number susceptibilities. We examine the technicalities associated with summing the Taylor series, and explore a Pade resummation. An examination of the Taylor series can be used to get an estimate of the location of the critical point in μ_B, T plane.

Keywords: quark number susceptibilities; QCD phase diagram; Taylor series and resummation; fluctuation and freezeout

---

1. Introduction

The phases of strongly interacting matter at different temperatures, T, and baryon chemical potential μ_B are of intense theoretical and experimental interest at present. Many contributions emphasized how the understanding of the physics of compact stars depend on quantum chromodynamics (QCD) at finite μ_B. In the experimental side, the beam energy scan (BES) runs in Relativistic Heavy Ion Collider (RHIC) experiment are trying to explore the phase diagram of QCD, and this is also the focus of the upcoming cold baryonic matter (CBM) experiment in the FAIR facility. Just as the equation of state of QCD at large T played a crucial role in the understanding of the ultrarelativistic heavy ion collisions in RHIC and LHC, the equation of state at $\mu_B > 0$ is important for the understanding of the BES and CBM experiment results. Unfortunately, it is highly nontrivial to reliably extract the equation of state for $\mu_B > 0$. For nonzero T but $\mu_B = 0$, numerical Monte Carlo simulations of lattice-discretized QCD allow one to calculate the equation of state nonperturbatively. But such techniques cannot be used directly at finite μ_B.

One way to get nonperturbative information about QCD at moderate μ_B is through a Taylor expansion in μ_B [1,2]; e.g., the pressure,

$$P(\mu_B, T) \;=\; P(0, T) \;+\; \sum_n \chi_B^n(T)\, \frac{\mu_B^n}{n!}. \tag{1}$$

The coefficients χ_B^n, called nonlinear baryon number susceptibilities, can be calculated nonperturbatively on lattice. We will present calculations of χ_B^n and discuss their interpretation. Then we will use the series Equation (1) to calculate the equation of state at moderate values of μ_B. An examination of the first few terms of the series indicate that the series expansion breaks down at some value of μ_B. We will argue that this is due to the presence of a critical point in the phase diagram in μ_B, T plane, and provide an estimate of its location.

One can, of course, introduce a chemical potential for each flavor of quark; e.g., for two flavors

$$P(\mu_B,T) - P(0,T) = \sum_{n_u n_d} \chi_{n_u n_d} \frac{\mu_u^{n_u}}{n_u!} \frac{\mu_d^{n_d}}{n_d!}, \qquad \chi_{n_u n_d} = \frac{\partial^{n_u+n_d} P}{\partial\mu_u^{n_u}\,\partial\mu_d^{n_d}}. \tag{2}$$

(For three flavors one will also have μ_s). The generalized quark number susceptibilities (QNS) can be easily connected to susceptibilities of conserved charges; e.g., μ_u and μ_d can be traded for the baryon number and isospin chemical potentials,

$$\mu_B = \frac{3}{2}(\mu_u + \mu_d), \qquad \mu_I = \mu_u - \mu_d. \tag{3}$$

The primary quantities we will calculate will be the QNS $\chi_{n_u n_d}$. We will use them to construct the χ_B^n using Equation (3), and then use Equation (2) to calculate thermodynamic quantities at finite μ_B.

The baryon number susceptibilities have been used to get information about the freezeout curve. In Section 3.3 we critically examine some issues that arise in such a comparison.

In Section 2 we briefly mention some technical details of our calculation. Our main results will be presented in Section 3. A summmary of the results, and their discussion, will be presented in Section 4. This report is based on Ref. [3], where more details can be found.

2. Calculational Details

We present results for a study of QCD with two degenerate flavors of staggered quarks. We use lattices with lattice spacing $a = 1/8T$, with quarks a little heavier than physical quarks (pion mass $\sim$ 230 MeV). We also compare our results with those from coarser lattices but similar fermion discretization [4]. Using the R algorithm [5] configurations were generated in the range 0.9 T_c–2 T_c. In this note T_c is used to indicate the crossover temperature at $\mu_B = 0$, as determined by the peak of the susceptibility of the Polyakov loop. The temperature scale is set using the Wilson flow observable w_0 [6] and two-loop running of the coupling.

Since our quark flavors are degenerate, $\chi_{lm} = \chi_{ml}$. Calculation of the higher order susceptibilities involve traces of products of matrices [7]. The traces were calculated with gaussian random vectors. A careful study of stability of the traces was done. It was found that in the region around T_c, the higher order susceptibilities stabilize only with a large number, $\sim$1000, of random vectors. We used 2000 vectors at these temperatures. At high temperatures results stabilize faster and 800 vectors were used. Our error estimates are based on a complete bootstrap analysis over the configurations and random vector sources.

3. Results

3.1. Quark Number Susceptibilities

The primary observables we measured were the generalized QNS. The baryon number susceptibilities can then be constructed from them. The QNS are interesting observables in their own right, as they reveal properties of the high temperature medium [8].

In Figure 1 we show some of the susceptibilities. In the left panel the diagonal susceptibilities $\chi_{n0}T^{n-4}$ of order $n = 2, 4, 6$ are shown. The second order susceptibility χ_{20} was the most interesting, and dominated the equation of state calculations at small μ_B. It was small in the hadronic phase and rose rapidly after T_c, behaving as an approximate order parameter. The approach to the Stefan–Boltzmann value was gradual. Note that this observable is known to have a strong lattice spacing dependence for the free theory; this can be traced to a particular operator which contributes only to this QNS [9]. It is therefore expected that at high temperatures, as one approaches the free theory, there will be considerable lattice spacing dependence for this observable. Taking the ratio of the lattice results with the corresponding lattice free theory results cancelled most of the cutoff effects, bringing the lattice results close to the perturbative results [10,11] by 2 T_c [12]. On the other hand, in the region around T_c, the results from $a = 1/8T$ and $a = 1/6T$ lattices agree quite well, indicating that cutoff effects were small in this regime [3]. The diagonal fourth order QNS χ_{40} approached perturbative results already by 1.5 T_c [12]. Close to T_c it deviated from perturbation theory and showed a peak structure. The parameter χ_{60} had a peak structure just below T_c, and became negligible just above T_c. These behaviors were consistent with trends seen in coarser lattices [13,14].

In the right panel of Figure 1 we show the results of the off-diagonal susceptibility χ_{ud}. In the hadronic phase, this observable was expected to be negative, as the u quark will be most often found together with a $\bar{d}$ in π^+. On the other hand, at high temperatures in the QGP phase, one would expect the u and d quark to be practically independent of each other, leading to $\chi_{ud} \sim 0$ [15,16]. As the figure reveals, χ_{ud} came very close to 0 by 1.1 T_c. In this figure we also show the results on a coarser lattice [4]. The cutoff dependence was small; the $N_t = 8$ results can therefore be expected to be close to the continuum results. This observable thus will severely constrain any model of quasibound structures in QGP at such temperatures.

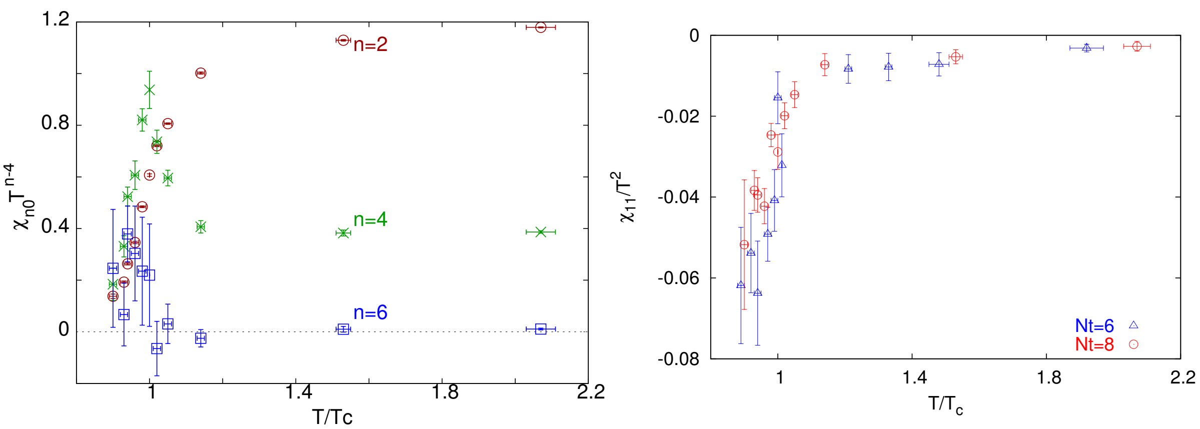

Figure 1. **(left)** The diagonal susceptibilities of order two, four and six, χ_{20}/T^2, χ_{40} and $T^2\chi_{60}$, in the temperature range 0.9–2 T_c. **(right)** χ_{11} in units of T^2, on lattices with $a = 1/8T$. Also shown for comparison are results for lattices with $a = 1/6T$.

Using the QNS, we can construct the baryon number susceptibilities χ_B^n using Equation (3). The results of the first three BNS are shown in Figure 2. These are also the coefficients appearing in the series expansion in Equation (1). For analysis of physics at finite μ_B, we convert Equation (1) into a series for $\chi_B^2(\mu_B)$. This series has a pole at the critical point (μ_B^E, T_E),

$$\frac{\chi_B^2(\mu_B, T_E)}{T_E^2} \sim \left(|\mu_B^2 - (\mu_B^E)^2|\right)^{-\psi} + \text{regularterms}. \tag{4}$$

A Taylor series expansion of χ_B^2 in μ_B will therefore break down at μ_B^E. An examination of the coefficients of the series gave us an estimate of the critical point in QCD phase diagram, $\frac{\mu_B^E}{T_E} = 1.85 \pm 0.04$, $\frac{T_E}{T_c} = 0.94 \pm 0.01$. These estimates, on lattices with $a = 1/8T$, agreed well with earlier estimates on coarser lattices with $a = 1/6T$.

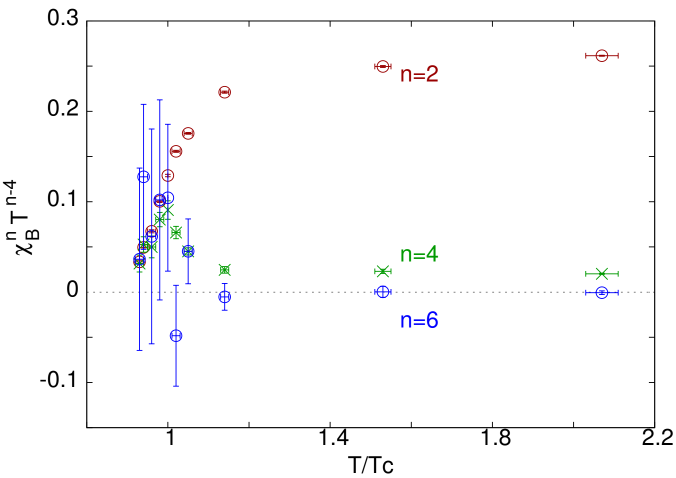

Figure 2. The baryon number susceptibilities of different order in the temperature range 0.9–2 T_c.

One cannot, of course, unequivocally predict a critical point from a finite series, less so a series with four noisy terms. The value above is our estimate of the location of the critical point, assuming the apparent finite radius of convergence is due to a critical region. Further confidence in this interpretation is gained from the fact that the series at T_E has all coefficients positive, as is required for the singularity to be on the real axis, for all bootstrap samples. We also found that the estimate of radius of convergence from ratios of different terms agree with each other [3]. Of course, the error quoted above, which is the statistical error obtained from a complete bootstrap analysis, is dominated by the ratio of the two smallest coefficients, i.e., χ_B^4/χ_B^2. We note that a recent determination of this ratio with improved quarks [17] is consistent with our ratio at 2σ level, though not at 1σ level.

Recent lattice studies, based on imaginary chemical potential, have reported on the lack of evidence for a critical point at small μ_B [18–20], while also commenting on the difficulty of putting a rigorous bound from these methods [20]. Note that the phase diagram in imaginary chemical potential is complicated; a more detailed investigation of the relation between computations in real and imaginary μ_B will be very important.

3.2. Equation of State at Finite μ_B

Using the baryon number susceptibilities, the equation of state can be obtained using Equation (1) and other series derived from it. Note, however, that the series will have very bad convergence properties as one approaches the critical region. On summing a finite ($\leq$4) number of terms in the series, one may therefore get a completely wrong result.

One way to improve the convergence of the series and to increase the sensitivity to the critical point is to use Pade resummation. In particular, a Pade resummation of

$$m_1 = \frac{\partial \log \chi_B^2/T^2}{\partial \mu_B/T} \sim \frac{\psi}{|\mu_B^2 - (\mu_B^E)^2|} + \text{regular}, \tag{5}$$

is expected to have much better convergence property in the critical region, where the singular term is dominant [9]. To get predictions at finite μ_B, we therefore do a Pade resummation of the series for m_1, and get other observables by integrating Equation (5). In order to study the convergence property of the resummation, we show in Figure 3a a comparison between results of the second order susceptibility obtained by resummation and by a direct summation of the series. At temperatures far from T_E, the two estimators are seen to agree. On the other hand, for the series at $T = T_E$ we see that the two differ considerably even at $\mu_B \ll \mu_B^E$. We expect the Pade resummed series to capture better the property of the series, and use it to extract observables at finite μ_B. Reassuringly, the μ_B^E from the Pade analysis agrees with that obtained from the radius of convergence analysis. See [3] for further details of the Pade analysis.

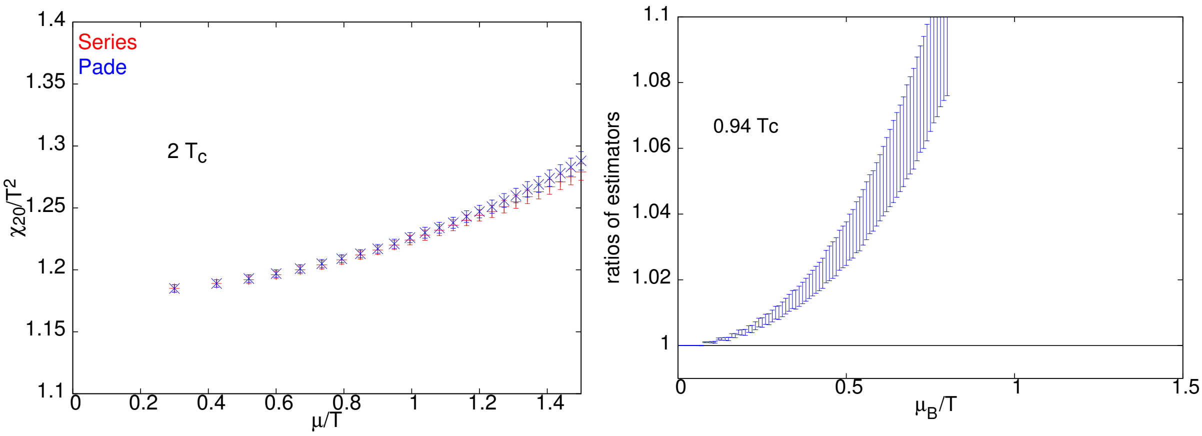

Figure 3. (**left**) Comparison of the Pade estimator for χ_{20} with the series-summed one at 2 T_c. (**right**) Ratio of the Pade estimator of χ_B^2 with the series summed one, at T_E = 0.94 T_c.

In the left panel of Figure 4 we show the results for χ_B^2 and $\Delta P(\mu_B, T) = P(\mu_B, T) - P(0, T)$ at the temperature $T_E = 0.94\, T_c$, obtained from successive integrations of the Pade approximant for m_1, Equation (5). The error bars are from a complete Bootstrap analysis for each observable. Note that the property of the impending breakdown of the series is captured in the Pade-resummed series by an explosion of the bootstrap error. This property has been noted before in Ref. [9], and is related to critical slowing down. This critical behavior gets successively milder as we do more integrations. In the figure we have shown the series for $T = 0.94\, T_c$, where the critical slowing down effect is strongest since it is our estimated temperature for critical endpoint. However, the effect of the critical point is seen also in other nearby temperatures.

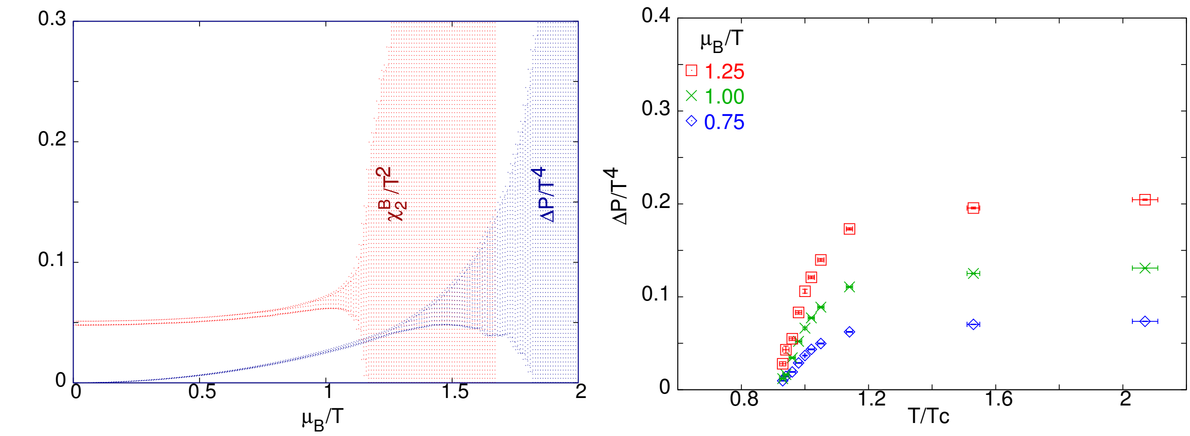

Figure 4. (**left**) The Pade-resummed results for pressure and χ_B^2 as function of μ_B, at $T = T_E$. (**right**) $\Delta P(\mu_B, T)$ as function of temperature, at various μ_B.

The figure shows that χ_B^2 is only mildly dependent on μ_B for $\mu_B < T$. As a result, the number density n is approximately linear and ΔP is approximately quadratic in μ_B. The right panel of Figure 4 shows our estimate of $\Delta P(\mu_B, T)$ at various values of $\mu_B < 1.25T$, i.e., away from the critical region. A more complete set of results, including those for the number density and the isotropic bulk compressibility, can be found in ref. [3]. As with χ_{20}, we expect that the cutoff effect is strong at high temperatures, and small in the temperature regime $T \lesssim T_c$. This can indeed be verified by comparing with the two flavor results from coarse lattices in [9].

3.3. Fluctuations and Freezeout

It has been suggested to use lattice observables like m_1 to determine the freezeout surface [21,22]. The parameter m_1, and other ratios of susceptibilities, are independent of the fireball volume. They can be connected to event-by-event fluctuations of net proton number if certain assumptions about the fireball are valid. The most important of these are: (a) the susceptibilities measured on the lattice are for the net baryon number. On the other hand, the fluctuations measured in the experiments are of the net proton number. For the comparison with the lattice susceptibilities to be meaningful, one needs to assume that the fluctuations of net baryon number are closely mimicked by those of the net proton number. (b) The fluctuation due to other, non-thermal sources need to be small compared to the thermal fluctuations. The underlying assumption that the system is always in thermal equilibrium up to T_c is probably too optimistic, especially as one comes closer to the critical region. We do not have anything specific to add about this, however. In what follows, we will assume that susceptibility ratios like m_1 mirror the experimental net proton fluctuations, and comment on some other systematics.

Quantities like m_1 are functions of μ_B, T; a comparison of such quantities with the corresponding experimental observables is expected to give us the parameters of the freezeout surface. While this idea has been used to map the freezeout surface from lattice [23,24], we would like to stress here the role of the critical region and associated breakdown of the series, Equation (1), in such an extraction. As we have discussed in the previous section, one needs to use a Pade resummation to get a reliable result and also to get an idea of the associated uncertainty in the series sum. To illustrate this, we have compared our results for m_1 with the corresponding fluctuation observable in the 200 GeV Au–Au runs from the STAR experiment. Taking the net proton fluctuation ratio $0.150 \pm 0.004 \pm 0.06$ [25] (the first error is statistical and the second, systematic), we have done a bootstrap analysis, taking the 68% confidence limit of the experimental observable and comparing with the lattice m_1. A single observable, m_1, cannot be used to specify both μ_B and T for the freezeout surface. In the literature, the freezeout temperature has sometimes been taken to be the chiral transition temperature, to extract μ_B. Instead of making such an assumption, we instead chart out a band in the μ_B, T plane using m_1. This is shown in Figure 5.

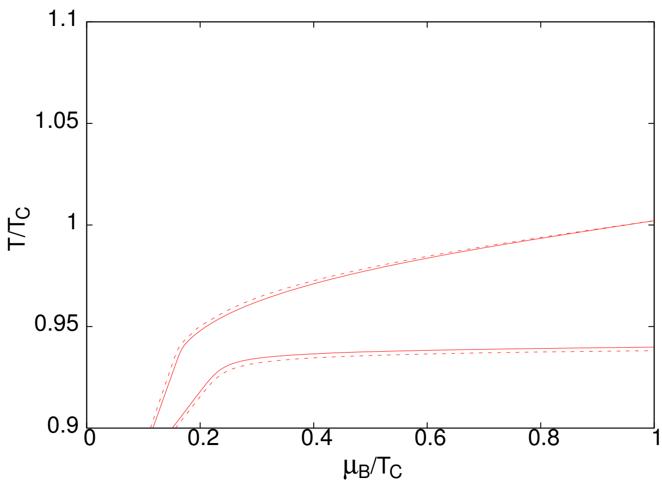

Figure 5. Estimation of the freezeout curve, from Pade estimation of m_1.

The first observation from Figure 5 is that after a small value of μ_B, the temperature dependence of the allowed band is very mild. Figure 5 indicates that the freezeout temperature is likely to be below T_c. The Pade-resummed series allows us to come to this conclusion based on m_1 alone. A finite series sum would, instead, have allowed temperatures above T_c [3]. The second observation from Figure 5 is that m_1 is not a good observable to constrain μ_B of the freezeout surface. In the literature, making the assumption that the freezeout temperature is the same as the chiral transition temperature, m_1 has been used to extract the freezeout μ_B for the STAR 200 GeV run. Our results show that if one uses the Pade resummed series, m_1 does not constrain μ_B very well in this temperature regime.

In the literature, the standard way to estimate the freezeout curve is by fitting the particle yields to a statistical hadronization model [26,27]. While such a fit has its own set of systematics, our discussion above suggests that the method based on lattice susceptibilities, while theoretically attractive, is at the moment not precise enough to replace it.

4. Summary and Discussion

In this report we presented results for quark number susceptibilities for two-flavor QCD on lattices with cutoff $a = 1/8T$, in the temperature range 0.9–2 T_c. Here T_c is the crossover temperature at $\mu_B = 0$ as determined by the peak of the Polyakov loop susceptibility. The major part of the cutoff dependence of susceptibilities at high temperatures can be understood from the cutoff dependence of the free theory. Interestingly, a strong coupling calculation of χ_{20} based on the gauge-gravity duality gives a result very different from QCD [28]. Close to T_c the QNS show sharp temperature dependence, which are very different from the behavior expected from perturbation theory. The off-diagonal susceptibility χ_{11} shows behavior consistent with weakly interacting quark-gluon plasma for $T > 1.1\,T_c$; this observable can be used to put strict constraints on models of quasibound structures in the QGP. A more detailed discussion of these and higher order QNS can be found in [3].

The QNS can be used to construct the n-th order baryon number susceptibilities χ_B^n. An examination of the first four (n = 2,4,6,8) BNS indicate a finite radius of convergence of the series expansion of $\chi_B^2(\mu_B)$. To estimate the location of a possible critical point in the phase diagram, we require that the series coefficients are all positive. Based on a bootstrap analysis, our estimate of the location of the critical point is $\frac{\mu_B^E}{T_E} = 1.85 \pm 0.04$, $\frac{T_E}{T_c} = 0.94 \pm 0.01$. The positivity of the series coefficients on all bootstrap samples give us confidence in our analysis. Note that the error is statistical and comes from an analysis of various ratios of χ_B^n, but it is dominated by the lowest ratio, i.e., χ_B^4/χ_B^2. The estimate of μ_B^E is consistent with the earlier estimate $\frac{\mu_B^E}{T_E} = 1.8 \pm 0.1$ from coarser lattice [4].

To get thermodynamic observables at finite μ_B, we use the series in μ_B. But since the series has finite radius of convergence, for μ_B close to this value a simple summing of the series will give inaccurate results. Following [9] we do a Pade resummation of the series for m_1 (Section 3.2). We find that the Pole in the Pade approximant matches the radius of convergence extracted from the series of χ_B^2. Successive integration of the series for m_1 then gives us the thermodynamic observables. We present results for pressure and number density in Section 3.2. We note that the finite radius of convergence of the series manifests itself in an explosion of the errorbar beyond a $\mu_B \sim T$. With more integrations, e.g., for pressure, the singularity becomes softer, resulting in the statistical error being in control to higher values of μ_B.

We also discuss connecting the susceptibility ratios like m_1 to ratios of event-by-event fluctuation observables, and attempt to estimate the freezeout curve using the experimental results for the latter. The issues in connecting susceptibility ratios to fluctuation ratios have been discussed in the literature. We investigate here a different issue: using the Pade resummed m_1 rather than the series resummed one, we find that the constraint put by m_1 on the freezeout μ_B is very weak. On the positive side, we find that the Pade resummed m_1 indicates by itself that the freezeout temperature is likely to be below T_c. Note that while this result is physically completely plausible to the point of sounding trivial, it has not always come naturally in freezeout determinations from statistical hadronization.

Author Contributions: The idea of Taylor expansion in μ_B is originally due to R.V.G. and S.G. All three authors have contributed in the work described here. This draft is the written version of S.D.'s talk in ICNFP 2018.

Funding: This research is a part of the ILGTI project funded by the Tata Institute of Fundamental Research (TIFR), Mumbai, an autonomous institution under Department of Atomic Energy, Govt. of India.

Acknowledgments: The computations described here were carried out using ILGTI, TIFR computing resources. We thank Ajay Salve and Kapil Ghadiali for technical support.

Conflicts of Interest: The authors declare no conflict of interest.

Abbreviations

The following abbreviations are used in this manuscript:

QCD	quantum chromodynamics
QGP	Quark-gluon plasma
BNS	Baryon number susceptibilities
QNS	Quark number susceptibilities
FAIR	Facility for antiproton and Ion Research
RHIC	Relativistic Heavy Ion Collider
CBM	Cold Baryonic Matter
BES	Beam energy scan
LHC	Large Hadron Collider

References

1. Gavai, R.V.; Gupta, S.; Ray, R. Taylor expansions in chemical potential. *Prog. Theor. Phys. Suppl.* **2004**, *153*, 270.
2. Ejiri, S.; Allton, C.R.; Hands, S.J.; Kaczmarek, O.; Karsch, F.; Laermann, E.; Schmidt, C. Study of QCD thermodynamics at finite density by Taylor expansion. *Prog. Theor. Phys. Suppl.* **2004**, *153*, 118.
3. Datta, S.; Gavai, R.V.; Gupta, S. Quark number susceptibilities and equation of state at finite chemical potential in staggered QCD with N_t=8. *Phys. Rev. D* **2017**, *95*, 054512.
4. Gavai, R.V.; Gupta, S. QCD at finite chemical potential with six time slices. *Phys. Rev. D* **2008**, *78*, 114503.
5. Gottlieb, S.A.; Liu, W.; Toussaint, D.; Renken, R.L.; Sugar, R.L. Hybrid Molecular Dynamics Algorithms for the Numerical Simulation of Quantum Chromodynamics. *Phys. Rev. D* **1987**, *35*, 2531.
6. Borsányi, S.; Durr, S.; Fodor, Z.; Hoelbling, C.; Katz, S.D.; Krieg, S.; Kurth, T.; Lellouch, L.; Lippert, T.; Mcneile, C.; et al. High-precision scale setting in lattice QCD. *JHEP* **2012**, *1209*, 010.
7. Gavai, R.V.; Gupta, S. The Critical end point of QCD. *Phys. Rev. D* **2005**, *71*, 114014.
8. Gottlieb, S.A.; Liu, W.; Toussaint, D.; Renken, R.L.; Sugar, R.L. The Quark Number Susceptibility of High Temperature QCD. *Phys. Rev. Lett.* **1987**, *59*, 2247.
9. Gupta, S.; Karthik, N.; Majumdar, P. On criticality and the equation of state of QCD at finite chemical potential. *Phys. Rev. D* **2014**, *90*, 034001.
10. Andersen, J.O.; Mogliacci, S.; Su, N.; Vuorinen, A. Quark number susceptibilities from resummed perturbation theory. *Phys. Rev. D* **2013**, *87*, 074003.
11. Haque, N.; Mustafa, M.G.; Strickland, M. Quark Number Susceptibilities from Two-Loop Hard Thermal Loop Perturbation Theory. *JHEP* **2013**, *1307*, 184.
12. Datta, S.; Gavai, R.V.; Gupta, S. QCD at finite chemical potential with N_t=8. *PoS Lattice* **2014**, *2013*, 202.
13. Gavai, R.V.; Gupta, S. Simple patterns for non-linear susceptibilities near T_c. *Phys. Rev. D* **2005**, *72*, 054006.
14. Ejiri, S.; Karsch, F.; Redlich, K. Hadronic fluctuations at the QCD phase transition. *Phys. Lett. B* **2006**, *633*, 275.
15. Koch, V.; Majumdar, A.; Randrup, J. Baryon-strangeness correlations: A Diagnostic of strongly interacting matter. *Phys. Rev. Lett.* **2005**, *95*, 182301.
16. Gavai, R.; Gupta, S. Fluctuations, strangeness and quasi-quarks in heavy-ion collisions from lattice QCD. *Phys. Rev. D* **2006**, *73*, 014004.
17. Bazavov, A.; Ding, H.T.; Hegde, P.; Kaczmarek, O.; Karsch, F.; Laermann, E.; Maezawa, Y.; Mukherjee, S.; Ohno, H.; Petreczky, P.; et al. The QCD equation of state to $\mathcal{O}(\mu_B^6)$ from Lattice QCD. *Phys. Rev. D* **2017**, *95*, 054504.
18. DÉlia, M.; Gagliardi, G.; Sanfilippo, F. Higher order quark number fluctuations via imaginary chemical potentials in N_f=2+1 QCD. *Phys. Rev. D* **2017**, *95*, 094503.
19. Vovchenko, V.; Steinheimer, J.; Philipsen, O.; Stoecker, H. Cluster Expansion Model for QCD Baryon Number Fluctuations: No Phase Transition at $\mu_B/T < \pi$. *Phys. Rev. D* **2018**, *97*, 114030.
20. Fodor, Z.; Giordano, M.; Guenther, J.N.; Kapas, K.; Katz, S.D.; Pasztor, A.; Portillo, I.; Ratti, C.; Sexty, D.; Szabo, K.K. Searching for a CEP signal with lattice QCD simulations. *arXiv* **2018**, arXiv:1807.09862.
21. Gavai, R.; Gupta, S. Lattice QCD predictions for shapes of event distributions along the freezeout curve in heavy-ion collisions. *Phys. Lett. B* **2011**, *696*, 459.

22. Gupta, S. Finding the critical end point of QCD: Lattice and experiment. *PoS CPOD* **2009**, *2009*, 025.
23. Bazavov, A.; Ding, H.T.; Hegde, P.; Kaczmarek, O.; Karsch, F.; Laermann, E.; Mukherjee, S.; Petreczky, P.; Schmidt, C.; Smith, D.; et al. Freeze-out Conditions in Heavy Ion Collisions from QCD Thermodynamics. *Phys. Rev. Lett.* **2012**, *109*, 192302.
24. Borsányi, S.; Fodor, Z.; Katz, S.D.; Krieg, S.; Ratti, C.; Szabo, K.K. Freeze-out parameters: lattice meets experiment. *Phys. Rev. Lett.* **2013**, *111*, 062005.
25. Adamczyk, L.; Adkins, J.K.; Agakishiev, G.; Aggarwal, M.M.; Ahammed, Z.; Alekseev, I.; Alford, J.; Anson, C.D.; Aparin, A.; Arkhipkin, D.; et al. Energy Dependence of Moments of Net-proton Multiplicity Distributions at RHIC. *Phys. Rev. Lett.* **2014**, *112*, 032302.
26. Petran, M.; Letessier, J.; Petráček, V.; Rafelski, J. Hadron production and quark-gluon plasma hadronization in Pb-Pb collisions at $\sqrt{s_{NN}}$ = 2.76 TeV. *Phys. Rev. C* **2013**, *88*, 034907.
27. Becattini, F.; Steinheimer, J.; Stock, R.; Bleicher, M. Hadronization conditions in relativistic nuclear collisions and the QCD pseudo-critical line. *Phys. Lett. B* **2017**, *764*, 241.
28. Petreczky, P. Lattice QCD at non-zero temperature. *J. Phys. G* **2012**, *39*, 093002.